

## Search for Extraterrestrial Intelligence with the ngVLA

C. NG <sup>1,2,3</sup> L. RIZK <sup>4</sup> C. MANNION <sup>5</sup> AND E. F. KEANE <sup>5,6</sup>

<sup>1</sup>*Dunlap Institute for Astronomy & Astrophysics, University of Toronto, 50 St. George Street, Toronto, ON M5S 3H4, Canada*

<sup>2</sup>*Department of Astronomy, University of California Berkeley, Berkeley CA 94720, USA*

<sup>3</sup>*SETI Institute, Mountain View, California, USA*

<sup>4</sup>*David A. Dunlap Department of Astronomy & Astrophysics, University of Toronto, 50 St. George Street, Toronto, ON M5S 3H4, Canada*

<sup>5</sup>*Centre for Astronomy, School of Physics, National University of Ireland Galway, University Road, Galway, H91 TK33, Ireland*

<sup>6</sup>*School of Physics, Trinity College Dublin, University of Dublin, College Green, Dublin 2, D02 PN40, Ireland*

(Received March 24, 2022)

Submitted to AJ

### ABSTRACT

The next generation Very Large Array (ngVLA) will be the premiere cm-wave radio array in the Northern hemisphere by the mid 2030s and thus has the potential to be one of the most effective instruments for the search for extra-terrestrial intelligence (SETI). We show that, as of now, the ngVLA will be the only facility capable of detecting an ETI signal generated by an Arecibo-like transmitter further than 300 pc. We present the optimal antenna array configurations and study the proposed frequency band coverage of the ngVLA and its implications to SETI. We argue for the ability to form of the order of 64 commensal high-spectral resolution beams, as the large number of line-of-sights is critical to provide a competitive survey speed when compared to other modern surveys with telescopes such as MeerKAT and the future SKA. We advocate an Ethernet-based telescope architecture design for the ngVLA, which will provide a high degree of flexibility in SETI data analysis and will benefit the wider astronomy community through commensal science and open-source code, maximizing the potential scientific output of the ngVLA.

*Keywords:* Interferometers (805) — Radio astronomy (1338) — Search for extraterrestrial intelligence (2127)

### 1. INTRODUCTION

The search for extra-terrestrial intelligence (SETI) is a sub-field of astrobiology concerned with the pursuit of observables that constrain the presence of intelligent life in the universe. Current efforts are focused on the detection of technosignatures—signs of non-human technology—whether intentionally or unintentionally transmitted by some intelligent form of life that is not our own. From its earliest conception in the 1960s, SETI research has been conducted primarily in the radio domain. Cocconi & Morrison (1959) first argued that one of our best chances of successfully detecting any extra-terrestrial intelligence (ETI) lies in radio emissions. Still today, radio searches are a good choice as a means of ETI detection from both a practical and a purely scientific point of view, as laid out in the “Nine Axes of Merit for Technosignature Searches” (Sheikh 2020), an analytical framework developed to assess the merits of any given SETI survey.

Electromagnetic radiation in the radio part of the spectrum remains a competitive strategy for information transfer over interstellar space. Unlike higher-frequency electromagnetic radiation, radio is not attenuated by dust extinction between us and any potential ETI. Radio receivers and transmitters, such as those developed here on Earth even before the age of space exploration, could also be easily within the engineering capabilities of any similarly advanced society. It is not unreasonable to assume that another technologically advanced civilization might arrive at the same conclusions as we have about the possibilities of the detection and/or transmission of radio waves over long distances.

In terms of the scientific nature of the potential discovery of a radio technosignature, there are further advantages. An intentional communicative radio transmission offers the unquestionably exciting advantage that, assuming we can decode such a signal, it will unambiguously answer the question of whether or not ETIs exist. It also requires no theorized extrapolation from current known technology or understanding of the laws of physics. Such a search runs the risk, however, of making potentially unfounded sociological assumptions about the nature of the extraterrestrial civilization in question, as it assumes a definite motivation for communication, see, e.g., [Wright \(2021\)](#).

From a practical standpoint, radio SETI is favoured for its cost-efficiency. Costs can be kept relatively low through commensal observation: piggybacking on telescope time without interfering with other projects running concurrently. The first example of commensal SETI dates back to the SERENDIP project ([Bowyer et al. 1983](#)), where a spectrum analyzer tapped into a split stream of intermediate-frequency band at the Hat Creek Radio Observatory. Further, upgraded versions of SERENDIP were then deployed on Arecibo and the Green Bank Observatories (see, e.g. [Chennamangalam et al. 2017](#)). Commensal observing arrangements are beneficial for the observatory in general, for instance in terms of telescope usage efficiency and scientific output. Any data gathered could also have ancillary benefits to other areas of astrophysical research such as the advances made by the Breakthrough Listen (BL) Initiative. For example, Fast Radio Bursts (FRBs) have been detected using both the BL digital backend at Green Bank ([Michilli et al. 2018](#); [Zhang et al. 2018](#); [Gajjar et al. 2018](#)) and during BL observations at Parkes ([Price et al. 2019](#)). It is well within our current technological capabilities, and without undue strain on available resources, to detect a radio signal from an ETI, if such a signal exists. It is one thing to find nothing because there is nothing there, but it is quite another thing, even from a purely objective standpoint, to find nothing because we did not look. As [Cocconi & Morrison \(1959\)](#) concluded: “The probability of success is difficult to estimate; but if we never search, the chance of success is zero.”

What exactly is the radio ETI signal we are looking for? Given that no convincing ETI detection has been made thus far, we do not definitively know the morphology and characteristics that might define a radio ETI signal. However, we can make an educated guess of what a potential ETI signal might look like by taking inspiration from human-made technosignatures observed in space. Fig. 5 in [Lebofsky et al. \(2019\)](#) shows the signal of the Voyager spacecraft as detected by the Green Bank telescope. This specific Voyager signal has a drift rate of 0.36 Hz/s, and is extremely narrow in spectrum. Human-made technology has frequently used filters to concentrate information in a narrow region of the spectrum, whereas astrophysical emissions tend to be a lot broader in bandwidth. [Siemion et al. \(2013\)](#) pointed out that emission no more than a few Hz in spectral width is an unmistakable indicator of engineering by an intelligent civilization, while only a fraction of a Hz worth of broadening is expected from the interstellar and interplanetary media. In order to detect narrow technosignatures like this, sensitive SETI projects require very high spectral resolution: collected data must have frequency bins on the order of 1 Hz. Another characteristic of the Voyager signal is the drift in its frequency over time as observed from an Earthbound receiver. This Doppler drift arises due to the relative acceleration between the receiver on Earth and the transmitter from space. In contrast, a stationary signal generated by human technology on the Earth’s surface would not have any differential drift rate. Thus far, the mainstream algorithm employed to search for these narrow-band drifting signals involve the use of the “tree de-Doppler” technique ([Siemion et al. 2013](#); [Enriquez et al. 2017](#); [Enriquez & Price 2019](#)).

Multiple larger-scale radio telescope projects are expected to come online in the next decade, which present exciting opportunities for SETI. Notably, the next generation Very Large Array (ngVLA; [Murphy 2018](#)) is going to be the premiere cm-wave radio array in the Northern Hemisphere and will improve by more than an order of magnitude the sensitivity and spatial resolution over the current Jansky VLA and the Atacama Large Millimeter/submillimeter Array (ALMA) at the same wavelengths. Here we assume the main SETI strategy on these telescopes is to maximize the number of stars monitored using beam formed data. Although going forward, one can look into the possibility of technosignatures unassociated with stars, for example in interstellar space. In this work, we present the results of studies into how the ngVLA can optimally perform SETI by maximizing the number of stars targeted. We analyze the antenna configuration (Section 2.2), compare different operational modes (Section 2.3) and study various beamformer capabilities offered by the ngVLA (Section 2.4). We present the target selection considerations in Section 2.5 and quantify the sensitivity of SETI with the ngVLA in Section 2.6. We argue for the need of an Ethernet-based telescope architecture in Section 2.7. In Section 3, we summarize the optimal SETI design for the ngVLA and propose indicative systems engineering design requirements that would enable these if adopted by the ngVLA.

## 2. THE NGVLA

### 2.1. Overview

93 The ngVLA is a proposed radio interferometer in the frequency range 1.2–116 GHz led by the National Radio  
 94 Astronomy Observatory (NRAO). It will be the Northern Hemisphere counterpart to the Square Kilometer Array  
 95 (SKA) ( $\lesssim 50$  GHz) and the Atacama Large Millimeter Array (ALMA) ( $\gtrsim 50$  GHz) in the South. The ngVLA will  
 96 provide 10 times the collecting area of the JVLA (Murphy 2018) as well as an order of magnitude improvement  
 97 on current observing capabilities in terms of both sensitivity and angular resolution. The ngVLA is a research  
 98 infrastructure project strongly endorsed by the Astronomy and Astrophysics Decadal Survey (Astro2020) of the U.S.  
 99 National Academy of Sciences. It will replace the JVLA as the U.S. flagship radio observatory by the mid 2030s when  
 100 commissioning is planned to be completed. As noted in Murphy (2018), the five key science goals of the ngVLA include  
 101 (1) unveiling the formation of solar system analogs on terrestrial scales, (2) probing the initial conditions for planetary  
 102 systems and life with astrochemistry, (3) charting the assembly, structure, and evolution of galaxies from the first  
 103 billion years to the present, (4) using pulsars in the Galactic Centre to test gravity theories, and (5) understanding  
 104 the formation and evolution of stellar and supermassive black holes in the era of multi-messenger astronomy. SETI  
 105 research has implications for both (1) and (2), but could also be considered a key science goal on its own, making it  
 106 relevant to the science strategy of the ngVLA.

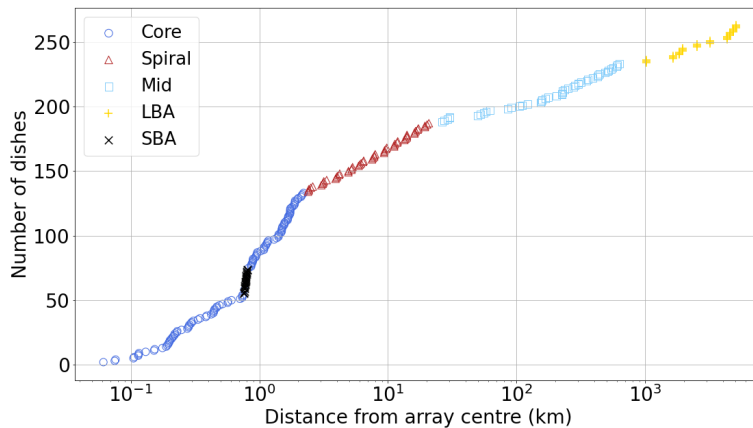


**Figure 1:** The size of the ngVLA array with respect to the number of antenna dishes. The reference antenna is taken to be that of the central antenna among the core array. The distance is calculated by taking the absolute distance from the  $x,y,z$  antenna coordinates.

## 107 2.2. Antenna configuration

108 Currently, the ngVLA antennas are not planned to be configurable like the VLA which means that the ngVLA  
 109 antennas will need to be located in a wide range of physical distances to fully sample various angular scales required  
 110 by the diverse science goals. See Fig. 1 for a visualization of the radial extent of the ngVLA dishes, based on the latest  
 111 antenna configuration (Rev. D) provided by C. Carilli. This up-to-date array layout can be found on the ngVLA  
 112 website<sup>1</sup>. At the time of writing, the ngVLA is designed to have 244 18-m antennas as well as 19 6-m antennas (Selina  
 113 et al. 2018). We created an interactive Google map of the positions of all the ngVLA antennas which can be found at  
 114 this link<sup>2</sup>. In summary, the ngVLA array is divided into three sub-arrays. Firstly, the Short Baseline Array (SBA) is  
 115 composed of all the 6-m dishes and contained entirely within the array core, approximately 1 km from the array centre.  
 116 Secondly, the Main Array (MA) is the main interferometric array and is made up of 214 18-m antennas. It can be  
 117 further divided into three parts: the core consists of 114 antennas in semi-random distribution within an approximately  
 118 2.2 km radius; the spiral sub-array consists of 54 antennas extending from the core in a five-armed spiral up to 20 km  
 119 from the array centre; and the mid-baseline array consists of the remaining 46 antennas in a five arms extending to  
 120 the south of the core with baselines from 30 to 700 km. Finally, further to the MA, there is the Long Baseline Array

<sup>1</sup> <https://ngvla.nrao.edu/page/tools>.

<sup>2</sup> <https://www.google.com/maps/d/edit?mid=1HT6MHwyt10tZWtMj2DwsqjXS1etn2HK5&ll=29.31924266678312%2C-114.9120717283779&z=4>

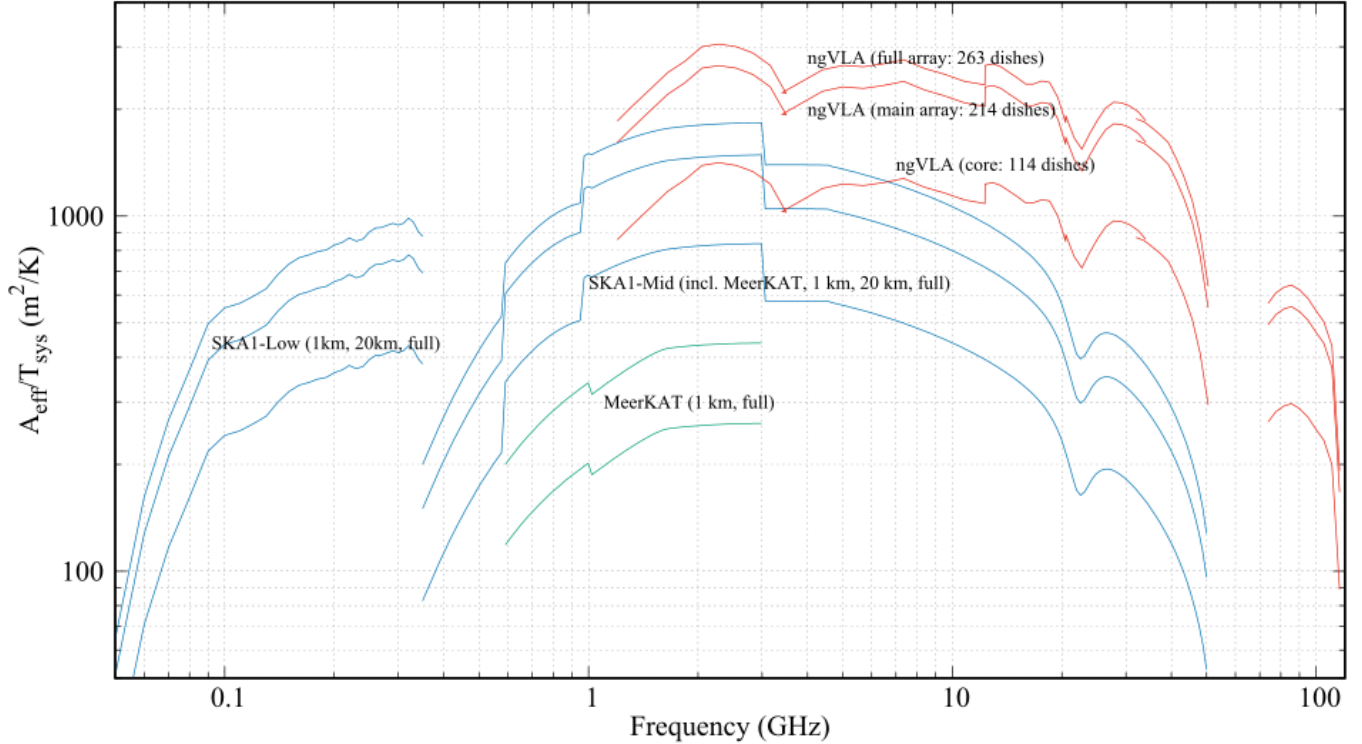


**Figure 2:** The sensitivity (y-axis) of ngVLA as compared to the SKA and MeerKAT, adapted from the top panel of Fig. 2 in Keane (2018). Three different curves for the ngVLA performance are shown, corresponding to using only 114 dishes from the core, 214 dishes from the MA, and 263 dishes from the full array. Three curves for the SKA1 are shown, corresponding to sub-arrays of diameter 1 km, 20 km and the full array (Braun et al. 2019). The ngVLA demonstrates the best sensitivity at high observing frequencies in all three antenna configurations shown.

121 (LBA), consisting of 30 18-m antennas located at stations on a continental scale, in Hawaii, Washington, California,  
 122 Iowa, West Virginia, New Hampshire, Puerto Rico, the US Virgin Islands, and Canada.

123 For SETI, having a dense configuration of antennas towards the centre is more desirable than including the very  
 124 long baselines of the LBA, assuming we prioritize larger field-of-view over high sensitivity of localized areas. While  
 125 the telescope sensitivity, defined as the effective area ( $A_{\text{eff}}$ ) over the system temperature ( $T_{\text{sys}}$ ), does increase with  
 126 increasing number of antennas (see Fig. 2), including long baseline antennas will reduce the synthesized beam size  
 127 and thus lower the sky coverage. In Fig. 3, we plot SETI survey speed against the distances of antennas from array  
 128 centre, where the survey speed is calculated as the field-of-view multiplied by gain to the power of  $\frac{3}{2}$  as suggested by  
 129 Equation 36 in Houston et al. (2021), given that the ETI signals we are after are not broadband by definition. We  
 130 can see that the ngVLA SETI survey speed is best when using antennas within about 1 km from the core. At its most  
 131 compact configuration D, the VLA has the largest beam size and thus systematically results in better survey speed  
 132 according to this calculation.

133

### 2.3. ngVLA Operational Model

134 NRAO has released an Envelope Observing Program (EOP)<sup>3</sup> (Wrobel et al. 2020), a notional prediction of how the  
 135 community might use the ngVLA during a typical year of full science operations. Based on the EOP, we show in Fig. 4  
 136 the fraction of time ngVLA will spend observing with each of its six receivers. A relatively high fraction of time will  
 137 be devoted to the higher frequency receivers, with the 93 GHz receiver being the most frequently used. For comparison,  
 138 we also studied the historic usage of the VLA between 2015 and 2019 inclusively. This observation log has been  
 139 obtained through processing of the META data associated with the commensal 340 MHz VLA Low-band Ionospheric

<sup>3</sup> [https://ngvla.nrao.edu/system/media\\_files/binaries/260/original/020.10.15.05.10-0002-REP-A-Notional\\_Envelope\\_Observing\\_Program.pdf?1600808616](https://ngvla.nrao.edu/system/media_files/binaries/260/original/020.10.15.05.10-0002-REP-A-Notional_Envelope_Observing_Program.pdf?1600808616)

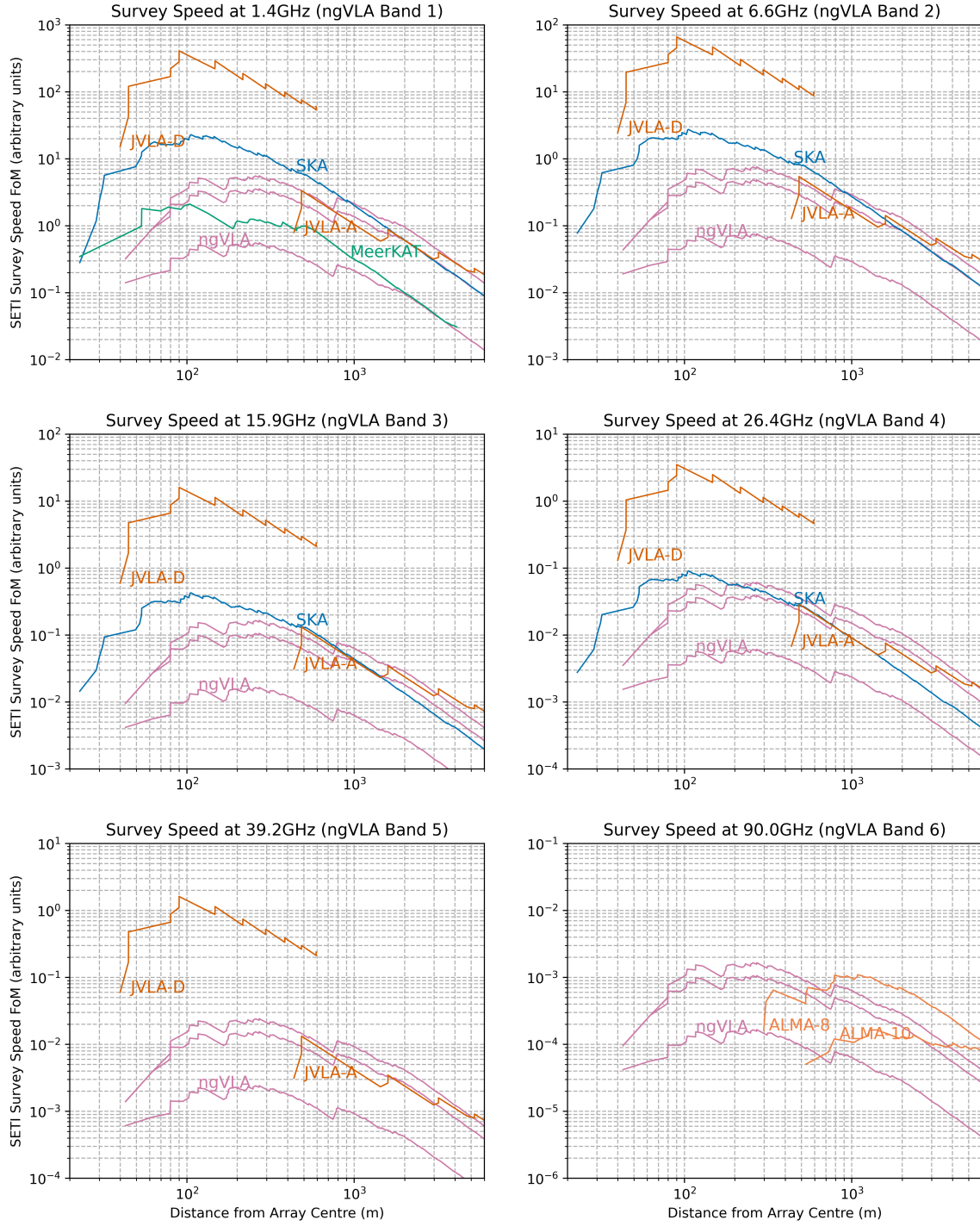


**Figure 3:** Survey Speed Figure of Merit (FoM) plots comparing ngVLA to the VLA A and D configurations, SKA Mid, MeerKAT and ALMA in each of its bands as a function of the antenna distances from the array centre. The ALMA  $T_{\text{sys}}$  is obtained from Fig. 4.7 in the ALMA Cycle 7 Technical Handbook (Remijan et al. 2019), where we assume a Precipitable Water Vapor (PWV) of 6 mm to match ngVLA data. The  $A_{\text{eff}}$  has been obtained from the ALMA Memo 602 and the antenna configuration from the online CASA simulator<sup>a</sup>. For the ngVLA and the SKA, these parameters can be found in our sensitivity calculator<sup>b</sup>. We use 64 SETI beams for the VLA and MeerKAT as suggested in Ng (2021) and Czech et al. (2021). For the ngVLA and the SKA, we include a curve with the same number of SETI beams for comparison. We also include a curve for 10 and 100 beams for the ngVLA, as these are potential scenarios as mentioned in Section 2.4. Note that the y-axis range is different in each panel to optimize for the specific value range.

<sup>a</sup> <https://almascience.nrao.edu/tools/casa-simulator>

<sup>b</sup> <https://github.com/evanocathain/ngVLA/blob/main/Sensitivity/functions.py>

and Transient Experiment (VLITE; Clarke et al. 2016). The JVLA only goes up to 50 GHz and the receiver band ranges are not exactly the same between ngVLA and the VLA for a direct comparison. Overall, we observe that the VLA spent more time at the lower frequency bands between 2015 and 2019 than what is proposed for the ngVLA.

Assuming a commensal SETI observing strategy, Fig. 4 gives us an idea of the frequency ranges we will be able to probe ETI transmission using the ngVLA. About one third of the time, the ngVLA will be observing at frequencies below 16 GHz, which overlaps with the so-called “terrestrial microwave window” (TMW). The TMW is the spectral region between 1 and 10 GHz identified as an ideal band for SETI by Morrison et al. (1977) due to the relatively low natural noise between the galactic synchrotron background ( $< 1$  GHz) and the emission and absorption by water and oxygen in the Earth’s atmosphere ( $> 10$  GHz).

The remaining two thirds of the time the ngVLA will be observing at high frequency windows. In Fig. 5, we plot the solid angle of the sky coverage vs observing frequencies for notable SETI surveys that were conducted in the past, are on-going, or are planned for the future. The sky coverage is calculated by multiplying the primary beam size with the number of pointings for a given observing frequency band. For reference, the whole sky represents a total solid angle of  $41,253 \text{ deg}^2$ . For the VLA, we use the exact number of pointings recorded during the five-year time span between 2015–2019. For the ngVLA, we assume the same number of pointings. Due to the large fraction of time the ngVLA will spend at high observing frequencies, SETI with the ngVLA will provide the best sky coverage from about 8 GHz upwards. The ngVLA will also observe in the  $\sim 100$  GHz window which has never been studied for ETI signals. In this sense, the ngVLA provides us with an opportunity to probe new, high frequency ranges where ETI signals could potentially be found. Indeed it has been suggested that ETIs might actually prefer to transmit in higher frequencies due to minimal scattering by the interstellar and interplanetary plasma (Benford et al. 2010). Although as pointed out earlier, our Earth’s atmosphere does make detection more challenging. Also, higher observing frequencies equate to smaller synthesized beam size and hence an overall slower survey speed (compare across the six panels in Fig. 3), which is another disadvantage when it comes to mapping the largest sky coverage.

Other notable spectral windows have been proposed for targeted SETI research. For example, the “water hole”—the band contained between the 1.420-GHz hydrogen line and the 1.667-GHz hydroxyl line—could be a quieter window in the radio spectrum and thus desirable for SETI surveys. Many hopeful SETI efforts focused on this bandwidth anticipating that an extraterrestrial civilization would recognize the significance and universality of water’s ions and deliberately use this frequency space to transmit a signal to other intelligent life. This frequency range will be covered by the ngVLA 2.4 GHz receiver, which spans a bandwidth between 1.2–3.5 GHz. Note that the 2.4 GHz receiver is only expected to be used about 8% of the time, so it would not provide a significant amount of data in the “water hole” spectrum.

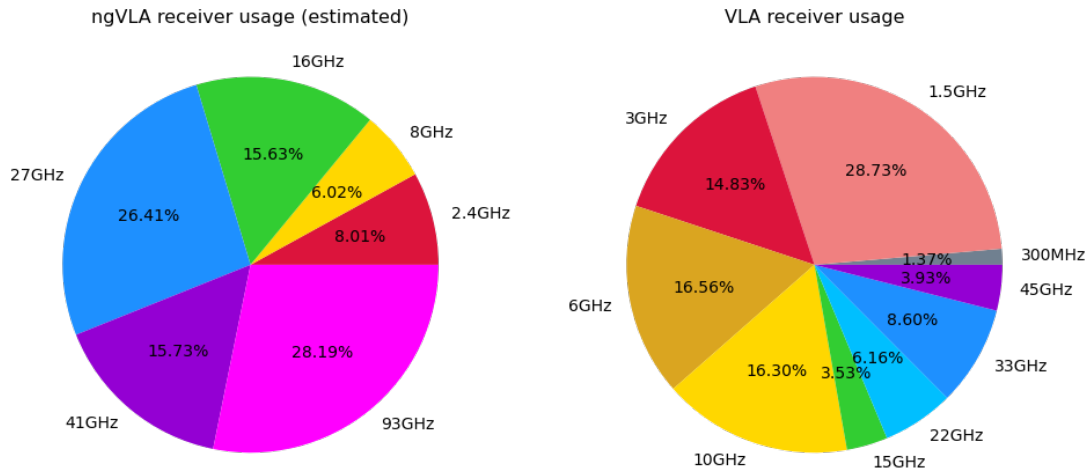


**Figure 4:** Comparison of (left) estimated ngVLA and (right) historical VLA receiver fractional usage time. We have used similar colours for receivers at comparable observing frequencies.

To better understand the survey completeness we can achieve with the ngVLA, another useful operational parameter to consider is the overall up-time of the telescope. While we will not have a concrete number until ngVLA comes online,

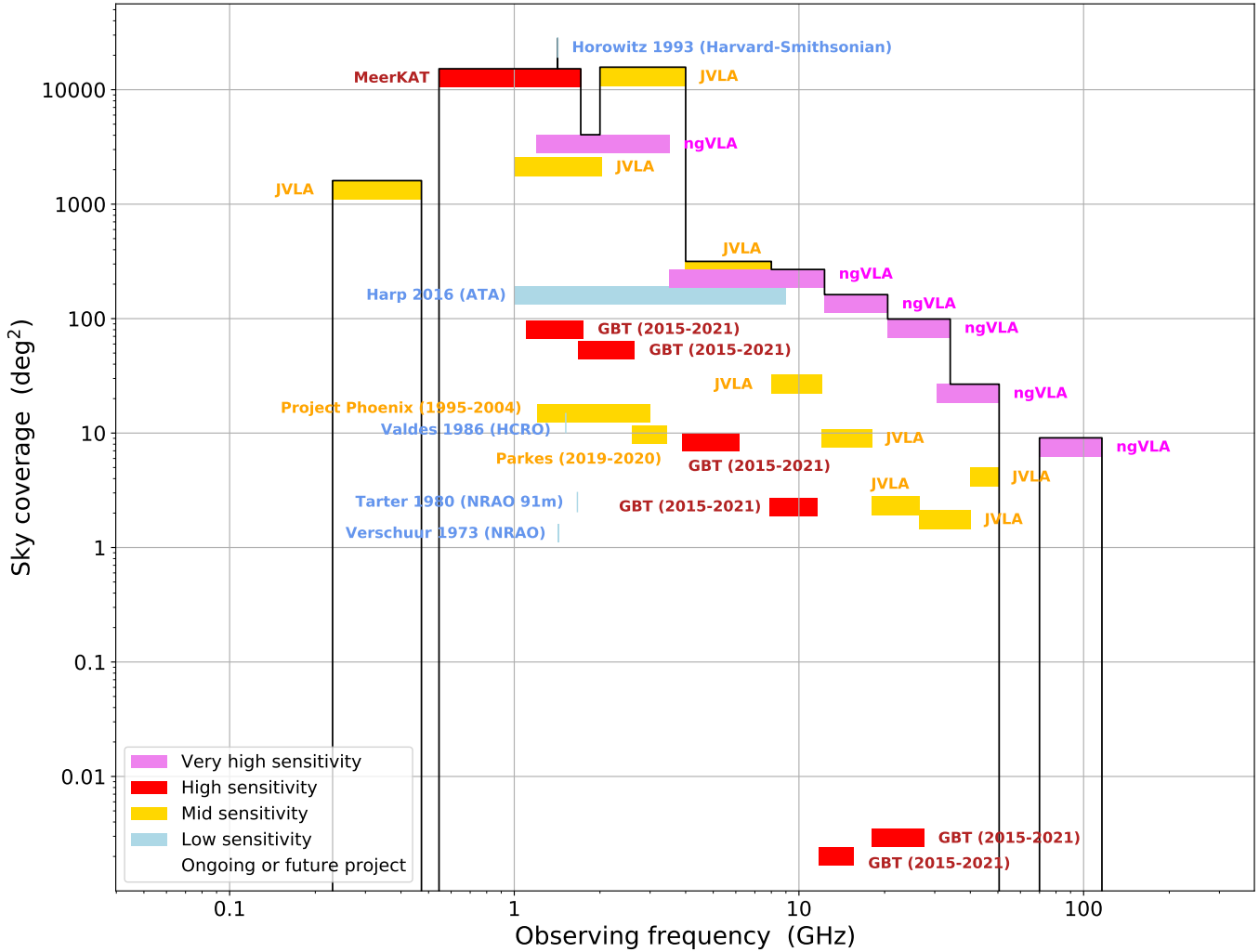


**Figure 5:** The sky coverage vs observing frequency for previous, ongoing, and proposed SETI surveys. Each project is colour-coded by one of four levels of sensitivity that show how far from Earth it can detect an Arecibo-like ( $10^{13}$ -W) transmitter signal, where  $d_* \leq 25$  pc is low sensitivity (light blue),  $d_* \leq 75$  pc is mid sensitivity (yellow),  $d_* \leq 250$  pc is high sensitivity (red) and anything above being very high sensitivity (purple). A SETI project with the ngVLA will span one of the largest sky coverage and observing bandwidth, while providing very high sensitivity capable of detecting an Arecibo-like transmitter beyond 250 pc from Earth.

173 we can again look into historical data from the VLA to get a handle on what we might be able to expect for the ngVLA.  
 174 According to Fig. 6, the VLA had an averaged up-time of 17.4 hours per day in 2015, which is about 70%. A similar  
 175 trend is observed in 2016–2019. This is comparable to most other radio observatories and we do not observe any  
 176 particular weekly or monthly pattern. We also looked into the cumulative pointing durations per unique source with  
 177 the VLA. From Fig. 7, we can see that many of the pointings are quite short and last for only tens of seconds (a  
 178 hundredth of an hour). These shorter pointings could be associated with calibration or test scans; if we were to  
 179 exclude these, we might expect typical dwell times to be on the order of a few minutes. The coloured lines show the  
 180 break-down distribution for each different year and overall the pattern is quite similar year to year. Assuming ETI  
 181 signals are persistent transmission and do not consist of discrete bursts, short pointing duration is undesirable to SETI  
 182 as it translates to a reduction in signal-to-noise that is proportional to the square root of the integration time, as  
 183 prescribed by the radiometer equation. For reference, other BL projects such as SETI with the Green Bank, Parkes,  
 184 or MeerKAT all have a minimum integration time of 5 min (Enriquez et al. 2017; Price et al. 2020; Czech et al. 2021).  
 185 A caveat, however, is that short pointings potentially means higher sky coverage, giving us more targets to monitor.

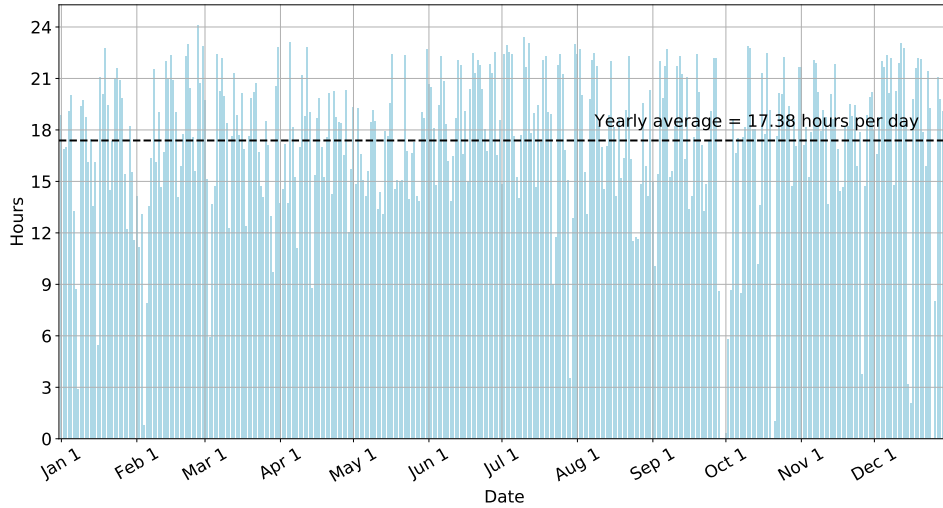


**Figure 6:** Observation time with the VLA in the year 2015. The yearly average of 17.38 hours per day is indicated by a dashed black line.

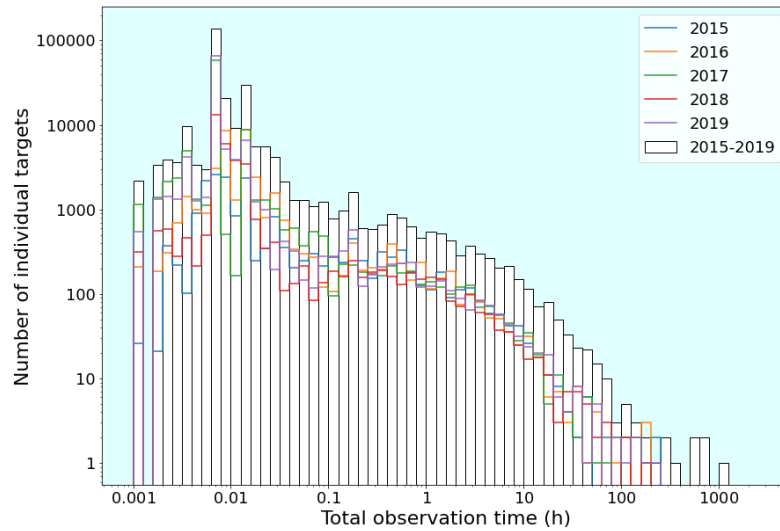


**Figure 7:** Observation time per individual target for all receivers on the VLA.

186

#### 2.4. *ngVLA beamformer*

187

188

189

190

191

192

193

194

195

196

The ngVLA Correlator and Beamformer (CBF) consists of two parts, the Very Coarse Channelizer (VCC) and the Frequency Slice Processors (FSPs). VCC splits the wideband input streams into narrower oversampled signals (sub-bands) called “frequency slices.” The coarse channelization at the VCC is computed using a polyphase filterbank and is the same for all observing modes (OMs). Subsequently, the FSPs independently process these frequency slides. The same frequency slice can be processed simultaneously at two different tridents compiler (Rupen et al. 2019) in the case of commensal observing with multiple OMs. At the time of writing, the planned ngVLA function OMs include correlation, very long baseline interferometry (VLBI) and pulsar beamforming (Ojeda et al. 2019). Two pulsar beamformer modes have been discussed, including an offline pulsar search OM and a pulsar timing OM. The pulsar search mode involves the use of phase-delay beamforming to form a larger number of beams. The delay is only truly compensated at boresight, while narrow band phase-delay approximations are used to synthesize beams towards other



offset directions within  $0.5^\circ$  from boresight. The beamforming aperture diameter is restricted to about 40 km from the core. Each beam will have a bandwidth of up to 8.8 GHz, which is the width of the widest receiver (Band 2). The ngVLA Reference Observing Program (ROF) explicitly specifies only 10 pulsar search beams, although of the order of 100 beams are required to cover the Galactic Centre through hexagonal packing and it is possible that a larger number of beams will be supported in the future.

The pulsar timing beams are voltage beams and are true-delay beamformed where Jones matrix corrections are applied per antennas. In [Carlson & Pleasance \(2018\)](#), it is stated that using the “Sparse config,” up to 4 beams can be generated per sub-array. The total beams  $\times$  bandwidth product is 4 beams/FSP  $\times$  50 FSPs  $\times$  200 MHz/FS = 40 GHz. This is applicable to the full array with any number of antennas and any aperture size. In principle, we can trade off a smaller bandwidth in order to form more coherent beams. For example, 50 coherent beams can be formed at 0.8 GHz/beam. Alternatively, the “Dense config” allows for 10 beams/FSP  $\times$  50 FSPs  $\times$  200 MHz/FS = 100 GHz, which means 50 beams at 2 GHz/beam can be formed. However, only a maximum of 144 antennas can be included in this configuration. In addition to these theoretical limits, the current technical requirements of the ngVLA central signal processor commit to a maximum of 10 pulsar timing beams with a maximum bandwidth of 8.8 GHz per beam ([Ojeda et al. 2019](#)). The goal of 50 beams is desired for globular clusters, but this is not currently required. A post-beamformer channelizer of up to 4k is possible, resulting in frequency resolution of the order of MHz.

For SETI, ideally we would need a new OM that is similar to the offline pulsar search mode with a much finer post beamformer channelizer that provides formed beams with Hz-wide channels. The large number of beams enabled by this enhanced offline pulsar mode is highly desirable for SETI as it increases our survey speed. From [Fig. 3](#), it can be seen that having 100 ngVLA SETI beams will provide comparable survey speed to SKA Mid. That fact that only antennas closest to the core can be incorporated is not an issue for SETI but rather a positive point, as discussed in [Section 2.2](#), the ngVLA survey speed peaks with antennas within about 1 km from the array centre. As stated in [Section 1](#), Hz-wide frequency resolution is typically required for SETI. In terms of the number of floating-point operations per second (flops) associated for the upchannelization operation, it scales with the length of the fine-channelization FFT, the number of polarizations, coarse frequency channels, antennas and the frequency resolution, which in theory will take on the order of several hundred Gflops per compute node based on the architecture of a 64-node compute cluster. Alternatively, SETI might be able to make use of the “Dense config” pulsar timing beams as is. We will however need to include a third stage channelizer in the downstream SETI engine to further channelizer the beams to Hz-wide resolution. The downside of piggybacking on the pulsar timing beams is the reduced survey speed. With only 10 beams, SETI on the ngVLA will be significantly slower than the on-going MeerKAT SETI project which has 64 commensal SETI beams ([Czech et al. 2021](#)). SETI would also be interested in analyzing incoherently formed beams which provide (reduced) sensitivity on the entire primary field of view. This might again require a new OM but should be relatively computationally inexpensive to produce.

### 2.5. Target selection

No technical memo is available at this stage regarding the predicted source scheduling on the ngVLA. The main SETI strategy on the ngVLA is to maximize the number of stars monitored via 24/7 commensal observing. For example, we can make use of the 32 million star catalog curated by [Czech et al. \(2021\)](#) to form a database, from which we can on-the-fly decide where to steer the SETI beams to point to stars within the primary field-of-view of the ngVLA. To first order, our priority is to observe stars based on their distances since, for a given transmitter power, closer targets will be more detectable. This target selection idea is based on the requirement that we have access to dedicated SETI beams. In the case that we piggyback to analyze the pulsar timing beams for example, then we would not have the luxury to choose where the beams are pointed to. That is another downside of using the pulsar timing beams for SETI; pulsar timing requires a subset of pulsars be monitored regularly, implying that the beams would be regularly returning to the same field-of-view instead of covering a large area of sky. We would, however, be able to set very stringent limits on the presence of ETI signals in those specific line-of-sights.

Other than covering the widest possible sky, there are regions of the galaxy that could be of greater interest to SETI and obtaining commensal observing time on those pointings would be of high priority. [Morrison & Gowanlock \(2014\)](#) proposed the idea of a “galactic habitable zone” (GHZ), a region around the Galactic Plane about  $60^\circ$  longitude and  $30^\circ$  latitude where they considered particularly attractive for extraterrestrial civilizations. Specifically, the line-of-sight towards the Galactic Centre has the largest integrated stellar density and could be a strategic place to conduct SETI ([Gajjar et al. 2021](#)). Commensal time with the ngVLA Galactic Centre pulsar search project (KSG4) is thus valuable

248 to SETI. The Earth Transit Zone (ETZ) is another potential SETI Schelling Point (Wright 2020), which describes  
 249 a region bracketing the ecliptic from which ETI would be able to observe our Earth transiting in front of the Sun  
 250 (Kaltenegger & Pepper 2020).

251

## 2.6. SETI Sensitivity

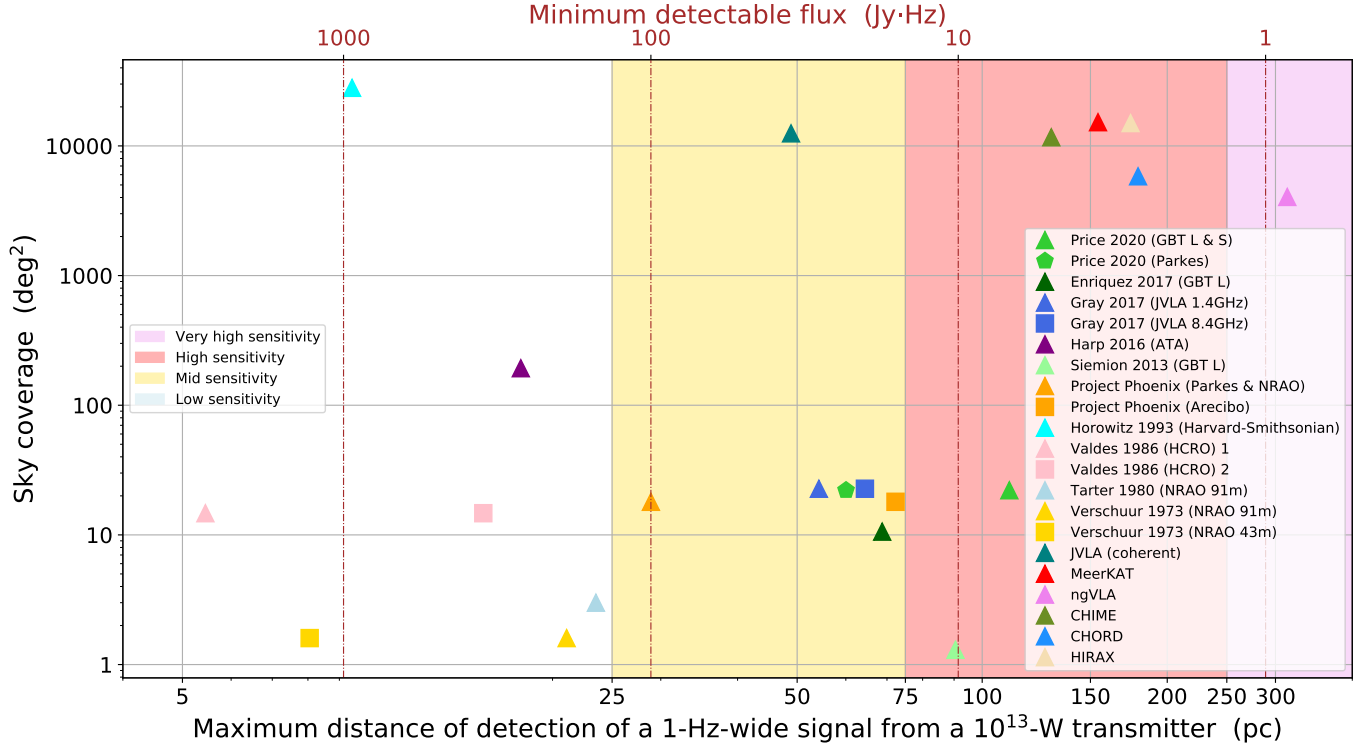


**Figure 8:** The sky coverage vs maximum distance of detection of an Arecibo-like transmitter. We obtain the parameters for other SETI projects from Enriquez et al. (2017). We categorize four levels of SETI sensitivity based on the maximum possible detection distance on the bottom x-axis, with  $\leq 25$  pc being low sensitivity (light blue),  $\leq 75$  pc being mid sensitivity (yellow),  $\leq 250$  pc being high sensitivity (red) and anything above being very high sensitivity (purple). The ngVLA is the only SETI project that can detect an Arecibo-like transmitter beyond 250 pc.

252 The ngVLA will complement SKA1-Low and SKA1-Mid as the only facilities with the capability to detect “leakage”  
 253 transmissions from omni-directional transmitters with power close to the brightest transmitters on Earth (Croft et al.  
 254 2018; Siemion et al. 2015). Here we attempt to further quantify the performance and expected survey sensitivity of  
 255 SETI with the ngVLA. The Arecibo radio telescope, before it was irreparably damaged in 2021, was the most powerful  
 256 planetary radar on Earth, capable of transmitting a pseudo-luminosity or an Equivalent Isotropic Radiated Power  
 257 (EIRP) of  $10^{13}$  W, as quoted by Enriquez et al. (2017). This is typically taken as a reference point of the strength of  
 258 ETI signal we can expect. Assuming an Arecibo-like transmitter that emits a 1-Hz-wide signal, based on the minimal  
 259 detectable flux ( $S_{\min}$ ) of a given telescope facility, we can work out the maximum distance ( $d_*$ ) the telescope can  
 260 detect the hypothetical ETI signal, where  $d_* = 10^{13}/(4\pi S_{\min})$ . In Fig. 5, we classify the SETI survey sensitivity into  
 261 four tiers, depending on how far the search could detect a 1-Hz-wide signal with the EIRP of Arecibo, where  $d_* \leq 25$  pc  
 262 is low sensitivity (light blue),  $d_* \leq 75$  pc is mid sensitivity (yellow),  $d_* \leq 250$  pc is high sensitivity (red) and anything  
 263 above being very high sensitivity (purple). This plot demonstrates how more recent and future searches are generally  
 264 greater in extent and in sensitivity. The ngVLA stands out for its superior sensitivity and its ability to better search  
 265 higher radio frequencies. Fig. 8 is a slightly different visualization which directly compares the sky coverage as a  
 266 function of (top horizontal axis) minimum detectable flux and (bottom horizontal axis) the maximum distance for the  
 267 detection of a 1-Hz-wide Arecibo-like signal. ngVLA’s most sensitive receiver (8-GHz receiver) would have the ability  
 268 to detect an ETI signal as far as just over 300 pc away. Considering our own galactic disc is over 30 kpc in diameter,

269 even our most ambitious search cannot yet look beyond our immediate neighbourhood for civilizations emitting signals  
 270 similar to our own.

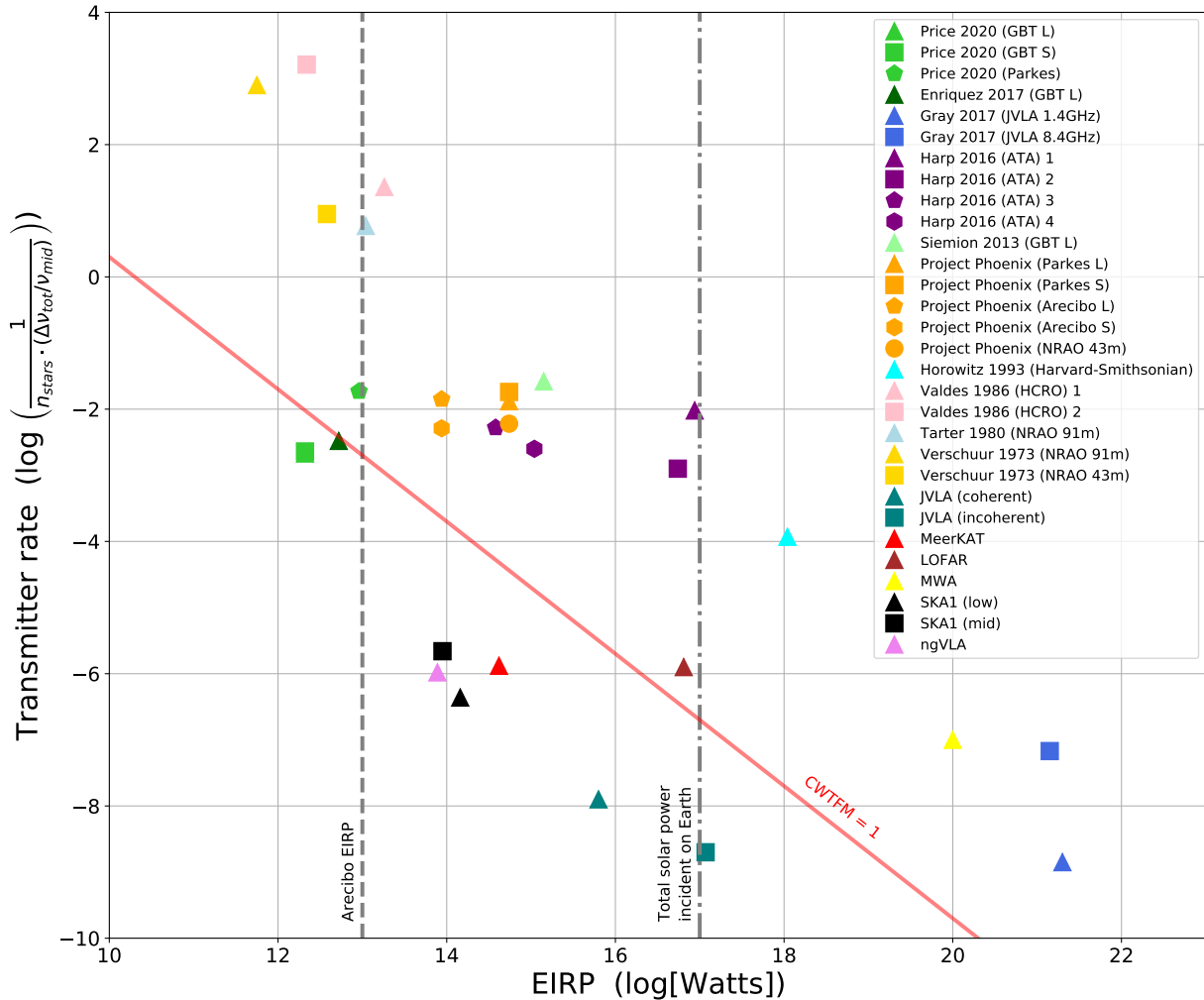


**Figure 9:** Transmitter rate vs EIRP for several SETI projects. The vertical lines indicate characteristic EIRP powers, while the dashed line represents the EIRP of the Arcsibo planetary radar and the dot-dashed line represents the total solar power incident on the Earth’s surface, also known as the energy usage of a Kardashev Type I civilization (Kardashev 1964).

271 Furthermore, we follow the recipes in Enriquez et al. (2017) to derive the EIRP of each SETI survey, which is defined  
 272 as  $4\pi d_{\text{max}}^2 S_{\text{min}}$ , where  $d_{\text{max}}$  is the distance to the farthest star studied by the specific survey and  $S_{\text{min}}$  is the minimum  
 273 detectable flux of the telescope. We also calculate the transmitter rate limit,  $(N_{\text{star}}(\frac{\nu_{\text{total}}}{\nu_{\text{centre}}}))^{-1}$ , where  $N_{\text{star}}$  is the  
 274 total number of stars studied by the project and  $\frac{\nu_{\text{total}}}{\nu_{\text{centre}}}$  is the fractional bandwidth of the receiver used. In the SETI  
 275 literature, the transmitter rate is often plotted on logarithmic axes against EIRP. Data points toward the bottom of  
 276 this plot represent surveys with large numbers of stellar targets and large fractional bandwidth; points toward the left  
 277 represent surveys where sensitivity is higher and distance to targets is lower. The dashed and dot-dashed vertical lines  
 278 represent the EIRP of the Arcsibo planetary radar, and total solar insolation, respectively. A transmitter rate of 1  
 279 would be an occurrence rate of 1 narrow band sinusoid per star, per GHz, at a centre frequency of 1 GHz. Most of the  
 280 survey parameters used in this plot can be found in Enriquez et al. (2017). For on-going and future SETI surveys, we  
 281 do not yet have a finalized  $d_{\text{max}}$  value. For MeerKAT, a  $d_{\text{max}}$  of 1 kpc is used (Czech et al. 2021). For JVLA coherent  
 282 and incoherent searches, we use 1 kpc and 825 pc respectively (D. Czech, priv. comm.). For LOFAR, we use 1000 ly (V.  
 283 Gajjar, priv. comm.). And we have assumed 4000 ly for both the ngVLA and the SKA. For these modern surveys, we

284 have conservatively assumed an  $N_{\text{star}}$  of 1 million. From Fig. 9, we can see that the ngVLA has one of the lowest EIRP  
 285 and transmitter rates and is comparable in performance to the SKA. We note that as a number of these parameters  
 286 are estimations, this plot should only be considered as an order of magnitude comparison. Nonetheless, these modern  
 287 projects are all below the red unity line of Continuous Waveform Transmitter Figure of Merit (CWTFM), providing  
 288 the most stringent limits on low-power radio transmitters around nearby stars.

### 289 2.7. Ethernet-based commensal observing

290 Over the last decade, the reduction in cost in commercial off-the-shelf (COTS) computing technology has enabled new  
 291 operation modes at radio observatories. As powerful CPU/GPU clusters become more affordable, there is an increasing  
 292 incentive in using data transport protocols such as Ethernet which easily interface with COTS hardware. Ethernet  
 293 provides for multiple subscribers using the multicast protocol, allows multiple subscribers to connect to a single raw  
 294 data stream, in turn providing more opportunity for scientific discoveries. An Ethernet-based architecture is also  
 295 flexible as expansion of the computing cluster can be relatively easily achieved by adding more switches. This is highly  
 296 desirable as the telescope can evolve with new research needs and can potentially benefit from the phased procurement  
 297 of hardware, which is likely to get cheaper over time. The importance of an Ethernet-based telescope capability is  
 298 highlighted in the Radio, Millimeter, and Submillimeter (RMS) panel report (Appendix M) of Astro2020. The recently  
 299 completed MeerKAT telescope in South Africa is the first to embrace a multicast Ethernet protocol (Camilo 2018)  
 300 for the transfer of all real-time data products. This architecture allows processing nodes to dynamically subscribe  
 301 to different types of data as needed. The scientific benefit of these commensal systems is clear, as the observational  
 302 data products get used in multiple ways in parallel. On MeerKAT, its success is demonstrated through a number  
 303 of commensal observing programs, which has led to the detection of FRB 121102 (Caleb et al. 2020) and the first  
 304 MeerKAT fast transient (Driessen et al. 2020). A similar effort is being commissioned for the VLA telescope through  
 305 the COSMIC (Commensal Open-Source Multimode Interferometer Cluster) project (Hickish et al. 2019). We strongly  
 306 advocate for an internal data transport protocol, such as Ethernet, on the ngVLA, which enables a multiple-data-  
 307 subscriber paradigm, and is easily supported by off-the-shelf data consumers such as standard CPU/GPU servers. This  
 308 will allow multiple subscribers to carry out multiple diverse research projects simultaneously, maximizing the potential  
 309 scientific output. With the flexibility of such Ethernet-based architecture, SETI projects could dynamically choose to  
 310 subscribe to existing pre-processed data products – like pulsar search beams, which provide an easy (and cost-effective)  
 311 route to add basic SETI capability to ngVLA – or unprocessed ADC samples, which provide full freedom in choosing  
 312 how to form beams at arbitrary frequency/time resolutions for SETI science. More importantly, the possibility of  
 313 accessing and storing snippets of raw voltages is particularly interesting to SETI projects, since that would give us the  
 314 ability to localize the ETI source provided a signal-of-interest is detected in the SETI beam, as is being deployed on  
 315 the MeerKAT and the VLA SETI projects. Commensal ngVLA data will no doubt also benefit the searches of other  
 316 transient objects such as FRBs and pulsars. Without an Ethernet-based commensal observing set up, each of these  
 317 projects will be competing for time on the ngVLA. High risk, high gain projects such as SETI might be turned down  
 318 in favour of research topics with low-lying fruits.

### 319 3. CONCLUSION

320 The ngVLA has the potential to be the most effective SETI instrument ever built. It is the only SETI system capable  
 321 of detecting an Arecibo-like transmitter beyond 300 pc, and will also provide one of the most stringent SETI limits  
 322 on low-power radio transmitters around nearby stars. In this work, we identify the SETI parameter space probed by  
 323 differing ngVLA configurations and consider the optimal ways of performing commensal SETI on the ngVLA. We find  
 324 that the best survey speed can be achieved by observing with only the core antennas about 1 km from the array centre.  
 325 Nominally according to the Envelope Observing Program, the ngVLA will spend one third of its time observing in  
 326 frequency bands compatible to the Terrestrial Microwave Window, although the majority of the time the ngVLA will  
 327 be observing at higher frequencies that have been underexplored by SETI projects thus far. That means the ngVLA  
 328 will provide the best SETI sky coverage above 8 GHz, while it will provide relatively little exposure around the “water  
 329 hole” spectrum at about 1 GHz. To integrate enough signal-to-noise when trying to detect a Doppler-drifting ETI  
 330 signal, we advocate for longer dwell time than what the VLA has historically used, ideally of the order of a few minutes  
 331 at least.

332 The main SETI strategy on the ngVLA is to maximize the number of stars monitored, therefore a large number of  
 333 coherently formed beams is highly desirable. For example, forming 64 SETI beams will give the ngVLA comparable

survey speed to the SKA-Mid. A new observing mode that is similar to the pulsar search mode but with high frequency resolution can help us achieve this. We can select stars based on the 32 million catalog curated by Czech et al. (2021), prioritizing for nearby stars. We might be able to use the 10 beams from the pulsar timing mode with an additional, third stage upchannelization, but the small number of beams would provide only comparable or worse survey speed as MeerKAT and will limit our targets to those chosen by the pulsar timing projects. SETI would also benefit from an additional observing mode of incoherent beam so that the entire primary field-of-view can be searched in parallel. Commensal observations at the Galactic Centre, the Galactic Habitable Zone, and the Earth Transit Zone are of particular interest as these sky regions are considered prime SETI locations. Finally, we echo the recommendation in Astro2020 and advocate for ethernet-based commensal observing capability on the ngVLA. Having access to raw voltages means we can localize signal-of-interest while snippets of data are still in the buffer and will allow more flexible SETI beamforming and visibility computations.

#### ACKNOWLEDGEMENTS

The work was funded by the National Radio Astronomy Observatory as part of the science community studies program for developing the ngVLA. LR was supported by the Summer Undergraduate Research Program (SURP) in astronomy & astrophysics at the University of Toronto. Construction and installation of VLITE was supported by NRL Sustainment Restoration and Maintenance funding. We thank Tracy Clarke for sharing the VLITE observation log, and we thank Chenoa Tremblay, Andrew Siemion, Kenneth Houston, Jack Hickish, David MacMahon and Savin Shynu Varghese for their useful comments and for carefully reading the manuscript.

#### APPENDIX

##### A. SOFTWARE

We have developed some software<sup>4</sup> to enable us to easily obtain metrics such as sensitivity and survey speed for different ngVLA sub-arrays for different lines of sight and observing conditions. This code can also be used to compare the ngVLA to the Square Kilometre Array (SKA, see e.g. Braun et al. 2019) and other relevant facilities.

#### REFERENCES

- Benford, J., Benford, G., & Benford, D. 2010, *Astrobiology*, 10, 475, doi: [10.1089/ast.2009.0393](https://doi.org/10.1089/ast.2009.0393)
- Bowyer, S., Zeitlin, G., Tarter, J., Lampton, M., & Welch, W. J. 1983, *Icarus*, 53, 147, doi: [10.1016/0019-1035\(83\)90028-3](https://doi.org/10.1016/0019-1035(83)90028-3)
- Braun, R., Bonaldi, A., Bourke, T., Keane, E., & Wagg, J. 2019, arXiv e-prints, arXiv:1912.12699. <https://arxiv.org/abs/1912.12699>
- Caleb, M., Stappers, B. W., Abbott, T. D., et al. 2020, *MNRAS*, 496, 4565, doi: [10.1093/mnras/staa1791](https://doi.org/10.1093/mnras/staa1791)
- Camilo, F. 2018, *Nature Astronomy*, 2, doi: [10.1038/s41550-018-0516-y](https://doi.org/10.1038/s41550-018-0516-y)
- Carlson, B., & Pleasance, M. 2018, in *Next Generation VLA Document No. TR-DS-000001*
- Chennamangalam, J., MacMahon, D., Cobb, J., et al. 2017, *ApJS*, 228, 21, doi: [10.3847/1538-4365/228/2/21](https://doi.org/10.3847/1538-4365/228/2/21)
- Clarke, T. E., Kassim, N. E., Brisken, W., et al. 2016, in *Society of Photo-Optical Instrumentation Engineers (SPIE) Conference Series*, Vol. 9906, Ground-based and Airborne Telescopes VI, ed. H. J. Hall, R. Gilmozzi, & H. K. Marshall, 99065B, doi: [10.1117/12.2233036](https://doi.org/10.1117/12.2233036)
- Cocconi, G., & Morrison, P. 1959, *Nature*, 184, 844, doi: [10.1038/184844a0](https://doi.org/10.1038/184844a0)
- Croft, S., Siemion, A., & Hellbourg, G. 2018, in *American Astronomical Society Meeting Abstracts*, Vol. 231, American Astronomical Society Meeting Abstracts #231, 342.24
- Czech, D., Isaacson, H., Pearce, L., et al. 2021, *PASP*, 133, 064502, doi: [10.1088/1538-3873/abf329](https://doi.org/10.1088/1538-3873/abf329)
- Driessen, L. N., McDonald, I., Buckley, D. A. H., et al. 2020, *MNRAS*, 491, 560, doi: [10.1093/mnras/stz3027](https://doi.org/10.1093/mnras/stz3027)
- Enriquez, E., & Price, D. 2019, turboSETI: Python-based SETI search algorithm. <http://ascl.net/1906.006>
- Enriquez, J. E., Siemion, A., Foster, G., et al. 2017, *ApJ*, 849, 104, doi: [10.3847/1538-4357/aa8d1b](https://doi.org/10.3847/1538-4357/aa8d1b)

<sup>4</sup> <https://github.com/evanocathain/ngVLA>

- 392 Gajjar, V., Siemion, A. P. V., Price, D. C., et al. 2018,  
393 ApJ, 863, 2, doi: [10.3847/1538-4357/aad005](https://doi.org/10.3847/1538-4357/aad005)
- 394 Gajjar, V., Perez, K. I., Siemion, A. P. V., et al. 2021, AJ,  
395 162, 33, doi: [10.3847/1538-3881/abfd36](https://doi.org/10.3847/1538-3881/abfd36)
- 396 Hickish, J., Beasley, T., Bower, G., et al. 2019, in Bulletin  
397 of the American Astronomical Society, Vol. 51, 269
- 398 Houston, K., Siemion, A., & Croft, S. 2021, AJ, 162, 151,  
399 doi: [10.3847/1538-3881/ac052f](https://doi.org/10.3847/1538-3881/ac052f)
- 400 Kaltenegger, L., & Pepper, J. 2020, MNRAS, 499, L111,  
401 doi: [10.1093/mnras/slaa161](https://doi.org/10.1093/mnras/slaa161)
- 402 Kardashev, N. S. 1964, Soviet Ast., 8, 217
- 403 Keane, E. F. 2018, in Pulsar Astrophysics the Next Fifty  
404 Years, ed. P. Weltevrede, B. B. P. Perera, L. L. Preston,  
405 & S. Sanidas, Vol. 337, 158–164,  
406 doi: [10.1017/S1743921317009188](https://doi.org/10.1017/S1743921317009188)
- 407 Lebofsky, M., Croft, S., Siemion, A. P. V., et al. 2019,  
408 PASP, 131, 124505, doi: [10.1088/1538-3873/ab3e82](https://doi.org/10.1088/1538-3873/ab3e82)
- 409 Michilli, D., Seymour, A., Hessels, J. W. T., et al. 2018,  
410 Nature, 553, 182, doi: [10.1038/nature25149](https://doi.org/10.1038/nature25149)
- 411 Morrison, I. S., & Gowanlock, M. G. 2014, in Search for  
412 Life Beyond the Solar System. Exoplanets, Biosignatures  
413 & Instruments, ed. D. Apai & P. Gabor, 5.4
- 414 Morrison, P., Billingham, J., & Wolfe, J. 1977, The Search  
415 for Extraterrestrial Intelligence, SETI., Vol. 419 (NASA -  
416 National Aeronautics and Space Administration (January  
417 1, 1977))
- 418 Murphy, E., ed. 2018, Astronomical Society of the Pacific  
419 Conference Series, Vol. 517, Science with a Next  
420 Generation Very Large Array
- 421 Ng, C. 2021, in The 2021 Assembly of the Order of the  
422 Octopus, 14, doi: [10.5281/zenodo.5160117](https://doi.org/10.5281/zenodo.5160117)
- 423 Ojeda, O., Lacasse, R., Selina, R., et al. 2019, in Next  
424 Generation VLA Document No.  
425 020.40.00.00-0001-REQ
- 426 Price, D. C., Foster, G., Geyer, M., et al. 2019, Monthly  
427 Notices of the Royal Astronomical Society, 486, 3636,  
428 doi: [10.1093/mnras/stz958](https://doi.org/10.1093/mnras/stz958)
- 429 Price, D. C., Enriquez, J. E., Brzycki, B., et al. 2020, AJ,  
430 159, 86, doi: [10.3847/1538-3881/ab65f1](https://doi.org/10.3847/1538-3881/ab65f1)
- 431 Remijan, A., Biggs, A., Cortes, P., et al. 2019, ALMA Doc,  
432 7
- 433 Rupen, M. P., Carlson, B., & Pleasance, M. 2019, in  
434 American Astronomical Society Meeting Abstracts, Vol.  
435 233, American Astronomical Society Meeting Abstracts  
436 #233, 361.06
- 437 Selina, R. J., Murphy, E. J., McKinnon, M., et al. 2018, in  
438 Astronomical Society of the Pacific Conference Series,  
439 Vol. 517, Science with a Next Generation Very Large  
440 Array, ed. E. Murphy, 15.  
441 <https://arxiv.org/abs/1810.08197>
- 442 Sheikh, S. Z. 2020, International Journal of Astrobiology,  
443 19, 237, doi: [10.1017/S1473550419000284](https://doi.org/10.1017/S1473550419000284)
- 444 Siemion, A., Benford, J., Cheng-Jin, J., et al. 2015, in  
445 Advancing Astrophysics with the Square Kilometre Array  
446 (AASKA14), 116. <https://arxiv.org/abs/1412.4867>
- 447 Siemion, A. P. V., Demorest, P., Korpela, E., et al. 2013,  
448 ApJ, 767, 94, doi: [10.1088/0004-637X/767/1/94](https://doi.org/10.1088/0004-637X/767/1/94)
- 449 Wright, J. T. 2020, International Journal of Astrobiology,  
450 19, 446, doi: [10.1017/S1473550420000221](https://doi.org/10.1017/S1473550420000221)
- 451 —. 2021, arXiv e-prints, arXiv:2107.07283.  
452 <https://arxiv.org/abs/2107.07283>
- 453 Wrobel, J. M., Mason, B. S., & Murphy, E. 2020, in Next  
454 Generation VLA Document No.  
455 020.10.15.05.10-0002-REP
- 456 Zhang, Y. G., Gajjar, V., Foster, G., et al. 2018, ApJ, 866,  
457 149, doi: [10.3847/1538-4357/aadf31](https://doi.org/10.3847/1538-4357/aadf31)